Catalytic Iron Metal Nanoparticles at Boron-Doped Diamond Electrodes: Sonoelectrochemical Deposition and Stripping

Veronica Saez[a], Jose Gonzalez-Garcia [a],

M. Anbu Kulandainathan[b], Frank Marken[c]*

[a]*University of Alicante, Department Quimica Fisica, Group Electroquim Aplicada, Ap Correos 99, Alicante, E-03080 Spain*

[b]*Central Electrochemical Research Institute, Karaikkudi, Tamil Nadu 630006 India*

[c]*Department of Chemistry, University of Bath, Bath BA2 7AY, UK*

To be submitted to Electrochemistry Communications

Abstract

A new methodology for the electro-deposition and stripping of highly reactive iron nanoparticles at boron-doped diamond electrodes is proposed. In aqueous 1 M NH_4F iron metal readily and reversibly deposits onto boron-doped diamond electrodes. The effect of deposition potential, FeF_6^{3-} concentration, deposition time, and mass transport are investigated. Power ultrasound (24 kHz, 8 Wcm^{-2}) is employed to achieve high mass transport conditions. Scanning electron microscopy images of iron nanoparticles of typically 20-30 nm diameter are obtained. It is shown that a strongly and permanently adhering film of iron can be formed and transferred into other solution environments.

The catalytic reactivity of iron nanoparticle deposits at boron-doped diamond is investigated for the reduction of trichloroacetate. The kinetically limited multi-electron reduction of trichloroacetate is dependent on the FeF_6^{3-} deposition and the solution composition. It is demonstrated that a stepwise catalytic reduction via dichloroacetate and monochloroacetate to acetate is feasible. This methodology in conjunction with power ultrasound offers a novel and versatile electro-dehalogenation methodology.

Keywords: iron, nanoparticle, boron-doped diamond, dehalogenation, remediation, ultrasound, sonoelectrochemistry, catalysis.

1. Introduction

Boron-doped diamond has found a wide range of applications in electrochemistry due to its outstanding material properties. In particular free-standing films of boron-doped diamond with high doping level have been employed to … The modification of the essentially inert boron-doped diamond surface has been employed in order to introduce specific catalytic activity for example with platinum [], x, and y []. The modification of boron-doped diamond with amine functionalities has been shown to dramatically change the reactivity towards oxygen. In this study the deposition of stable deposits of iron and iron oxides is demonstrated to give a novel catalytic reactivity to boron-doped diamond electrode surfaces.

Several previous studies have addressed the application of boron-doped diamond in stripping analysis and in particular in cathodic stripping voltammetry employing anodic deposition of metal oxides.

Iron nanoparticles are known to be highly reactive and they have been employed in processes such as dehalogenation and remediation [[1]] or nickel sequestration [[2]]. The reduction of halogenated methanes [[3]], trichloroethane [[4]], environmental DDT [[5]], and poly-chlorinated biphenyls [[6]]. Nanoscale zero valent colloidal iron has also been proposed for the removal of arsenic from drinking water [[7]]. … The use of iron nanoparticles deposited at electrode surfaces has been reported very rarely and the lack of this kind of approach has been pointed out in a recent review [8]. In part this lack of study in this important field is due to the high reactivity of iron deposits and the rapid formation of inert oxide coatings. However, in this study it is demonstrated

that in the presence of fluoride both the high reactivity and the formation of oxide coatings can be utilized. Conventional anodic stripping voltammetry with trace amounts of iron is possible and iron deposits at boron-doped diamond electrodes are durable and catalytically very active.

Complexes of iron and fluoride are readily formed

The effect of fluoride anions on the surface chemistry of iron and iron oxides (hematite) has been studied.

This study addresses an important aspect of iron nanoparticle decorated boron-doped diamond electrodes and their reactivity. The deposition procedure and the demonstration of catalytic reactivity in this report will be of considerable use in the utilization of iron redox catalysis.

2. Experimental

2.1. Chemical Reagents

NH4F, Fe(NO3)3, EDTA, Dithionite, trichloroacetate, dichloroacteate, monochloroacetate, Demineralised and filtered water of resistivity not less than 18 MOhm cm was taken from an Elga water purification system. Argon (Pure shield, BOC) was employed for de-aeration of electrolyte solutions.

2.2. Instrumentation

Scanning electron microscopy images were obtained on a JEOL JSM6310 system. A conventional three-electrode micro-Autolab III potentiostat system (Eco Chemie, NL)

was employed to control the potential at the working electrode. The counter electrode was a platinum gauze (1 cm^2) and the reference electrode was a saturated Calomel electrode, SCE, Ref 401, Radiometer). The working electrode 3 mm diameter boron-doped diamond electrode (Windsor Scientific, UK) and in some cases a 3 mm diameter glassy carbon electrode (BAS, USA).

Sono-electrochemical measurements were conducted in a 100 mL three-necked cell with the working electrode fixed and opposite to the ultrasonic glass horn probe which is immersed from the top of the cell [31]. An ultrasonic processor (Hielscher UP 200 G, 24 Hz, 200W, maximum ultrasound intensity 8 Wcm^{-2}) with a 13 mm diameter glass horn was employed. The electrode to horn distance was kept constant at 5 mm and the maximum ultrasound intensity, 8 Wcm^{-2}, was applied in all experiments. Ultrasound was only applied for short periods of time to prevent the temperature of the solution in the electrochemical cell from rising above room temperature ($T = 24 \pm 4\ ^oC$). High puritiy argon (BOC) was employed to thoroughly de-aerate all solutions prior to experiments.

2.3. Sonoelectrochemical Mass Transport Calibration

In order to quantify mass transport effects introduced by ultrasonic agitation, a calibration procedure has been developed. The $Fe(CN)_6^{3-/4-}$ redox system provides a reversible one-electron reference system in aqueous 1 M NH_4F. Figure 1A shows a typical cyclic voltammogram obtained for the reduction and re-oxidation of 5 mM $Fe(CN)_6^{3-}$ in 1 M NH_4F at a 3 mm diameter boron-doped diamond electrode. The reversible potential is 0.25 V vs. SCE and the peak-to-peak separation 76 mV at a scan rate of 0.2 Vs^{-1} consistent with almost reversible electron transfer. A plot of the cathodic peak current versus the square root of scan rate is linear and allows the diffusion

coefficient for the $Fe(CN)_6^{3-}$ anion, $D_{Fe(CN)_6^{3-}} = 0.48\ (\pm 0.02) \times 10^{-9}\ m^2 s^{-1}$, to be obtained [9]. Next, chronoamperograms were recorded in order to determine the mass transport controlled limiting current under ultrasound conditions and as a function of the electrode to horn distance (see Figure 1B). The mass transport coefficient, k_m, based on equation 1 was determined and is plotted versus the electrode to horn distance in Figure 1C.

$$i_{\text{lim}} = n F k_m c \qquad (1)$$

In this equation i_{lim} is the average mass transport controlled limiting current density, n is the number of electrons transferred per molecule diffusing to the electrode surface, F is the Faraday constant, and c is the bulk concentration of $Fe(CN)_6^{3-}$.

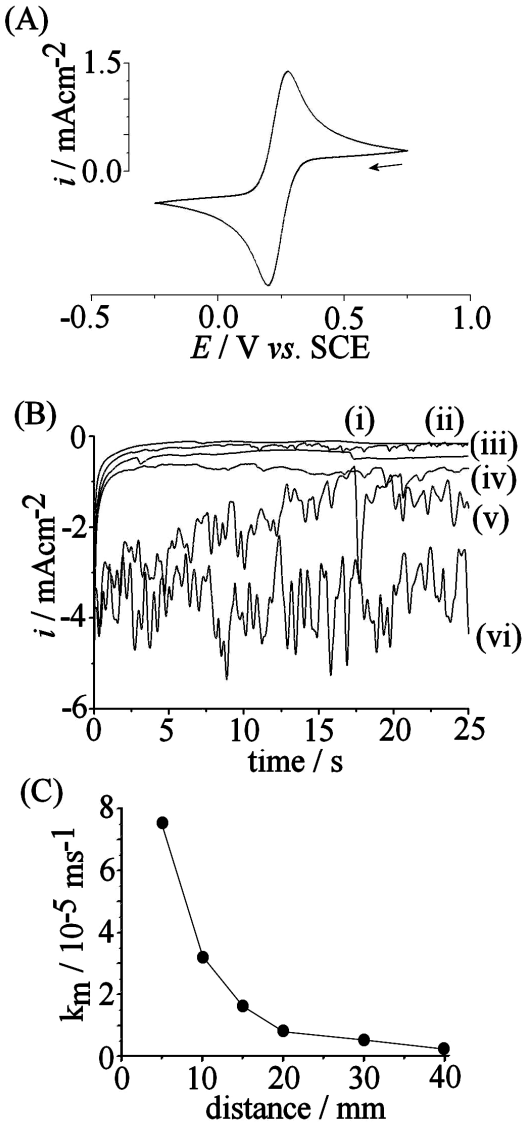

Figure 1. (A) Cyclic voltammogram (scan rate 0.2 Vs^{-1}) for the reduction and re-oxidation of 5 mM $Fe(CN)_6^{3-}$ in aqueous 1 M NH_4F at a 3 mm diameter boron-doped diamond electrode. (B) Chronoamperograms (applied potential 0.1 V vs. SCE, 8 Wcm^{-2} ultrasound) for the reduction of 5 mM $Fe(CN)_6^{3-}$ in aqueous 1 M NH_4F with an electrode to horn gap of (i) 40, (ii) 30, (iii) 20, (iv) 15, (v) 10, and (vi) 5 mm. (C) Plot of the average mass transport coefficient obtained from the limiting current (8 Wcm^{-2} ultrasound) versus the electrode to horn tip distance.

From the calibration data it can be seen that good mass transport enhancement effects are observed for an electrode to horn distance of 5 mm with $k_m = 7.5 \times 10^{-5}$ ms^{-1}. All sonoelectrochemical experiments in this study were conducted with this electrode to horn distance. With the diffusion coefficient $D_{Fe(CN)_6^{3-}} = 0.48 \times 10^{-9}$ m^2s^{-1} known, it is

possible to obtain an estimate for the diffusion layer thickness $\delta = \frac{D_{Fe(CN)_6^{3-}}}{k_m} = 6.4$ μm. This value is in good agreement with literature reports [10,11] and consistent with strong mass transport enhancement.

2.4. Cleaning Procedure for the Removal of Iron from the Boron-Doped Diamond Electrode Surface

After repeated use in iron stripping voltammetry experiments it was observed that iron remained immobilized at the electrode surface. Nitric acid (prolonged exposure to hot or cold 0.5 M HNO_3) did not remove the deposits and well defined residual stripping peaks were observed in the absence of FeF_6^{3-} in solution. However, immersion of the electrode into a solution of 10 mM sodium dithionite and 100 mM EDTA overnight completely removed iron and resulted in a clean background voltammogram in aqueous 1 M NH_4F.

3. Results and Discussion

3.1. The Electro-Deposition and Stripping of Iron: Reactivity in Aqueous Fluoride Media

A clean boron-doped diamond electrode immersed in aqueous 1 M NH_4F solution containing 10 μM FeF_6^{3-} shows a well defined stripping response at -0.58 V vs. SCE after scanning the potential to -1.5 V vs. SCE (see Figure 2). In the absence of FeF_6^{3-} no peak is observed and by varying the FeF_6^{3-} concentration (see below) the peak

feature can be clearly identified as iron stripping. The process is tentatively assigned to a three electron process (equation 2, vide infra).

$$Fe(metal) + 6\ F^-(aq) \longrightarrow FeF_6^{3-}(aq) + 3\ e^- \qquad (2)$$

The process is highly sensitive to low concentrations of iron (down to sub-μM concentrations) and requires both (i) the boron-doped diamond electrode and the presence of 1 M NH_4F. Equivalent experiments with a glassy carbon working electrode or with lower concentrations of NH_4F were not successful. When conducted in the presence of ultrasound, the mass transport enhancement of the cathodic process can be seen (see Figure 2 curve iii).

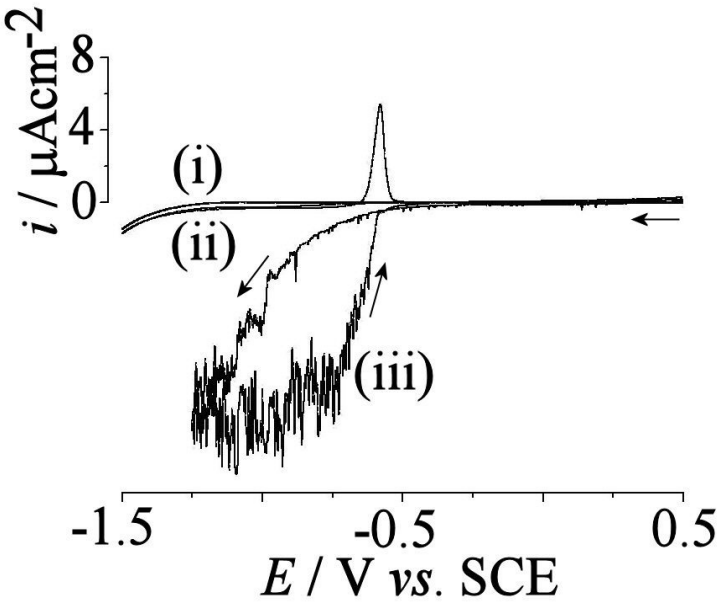

Figure 2. Cyclic voltammograms (scan rate 0.02 s^{-1}) obtained at a 3 mm diameter boron-doped diamond electrode in aqueous 1 M NH_4F: (i) background, (ii) in the presence of 10 μM FeF_6^{3-}, (iii) in the presence of 10 μM FeF_6^{3-} and 8 Wcm^{-2} ultrasound (5 mm horn to electrode distance).

The cathodic current in the presence of ultrasound increases rapidly and at potentials of ca. -1 V vs. SCE the increased noise level (due to turbulent convection) is indicative of mass transport control. The limiting current observed after reversal of the scan direction can be analysed based on equation 1 to give the approximate number of electrons transferred in this process. From the average limiting current density of 10 μAcm^{-2} and k_m = 7.5 × 10-5 ms^{-1} the number of electrons transferred, n ≈ 1 is obtained. The process is consistent with the one electron reduction of FeF_6^{3-} (see equation 3).

$$FeF_6^{3-}(aq) + e^- \rightleftharpoons FeF_6^{4-}(aq) \quad (3)$$

This process is not observed at the bare boron-doped diamond electrode and it is likely that this process is catalysed by the presence of iron metal or iron oxide at the electrode surface. From data in Figure 2 the reversible potential for the $FeF_6^{3-/4-}$ redox system can be estimated as ca. -0.6 V vs. SCE. Interestingly, the peak feature for the irons tripping process is suppressed in the presence of ultrasound presumably due to the fast mass transport leading to rapid comproportionation (see equation 4) under fast mass transport conditions.

$$Fe(metal) + 2\ FeF_6^{3-}(aq) \rightleftharpoons 3\ FeF_6^{4-}(aq) \quad (4)$$

Due to the intermediate Fe(II) species, iron stripping processes are more complicated when compared to simple electrochemical stripping processes. The direct stripping of the iron deposit to give the reduced form FeF_6^{3-} at a more negative potential appears

unfavorable either due to a kinetic effect or due to the reversible potential for the Fe/FeF_6^{4-} system being more positive compared to the Fe/FeF_6^{3-} system.

3.2. The Electro-Deposition and Stripping of Iron: Deposition Potential and Time Effects

Next, the effect of the deposition potential on the stripping peak feature is investigated. Linear scan voltammetry experiments are performed with a 30s deposition time followed by a scan to positive potentials. Figure 3A shows that the iron stripping peak is characteristically dependent on the deposition potential. The peak is observed at a deposition potential of -1 V vs. SCE and a systematic increase is seen at more negative deposition potentials. However, a complication arises at potential negative of -1.6 V vs. SCE where the stripping peak broadens. The reason for the broadening is currently unknown but it can be avoided in the presence of ultrasound.

In the presence of ultrasound (24 kHz, 8 Wcm^{-2}, 5 mm electrode to horn distance) a much improved stripping peak is detected. In contrast to data shown in Figure 2, here the deposition process is more dominant and loss of the stripping signal due to comproportionation can be ruled out. Due (at least in part) fast mass transport the stripping peaks are typically 50-fold increased and highly symmetric even at more negative deposition potentials. A mass transport limit for the iron deposition process is not reached even at -2 V vs. SCE.

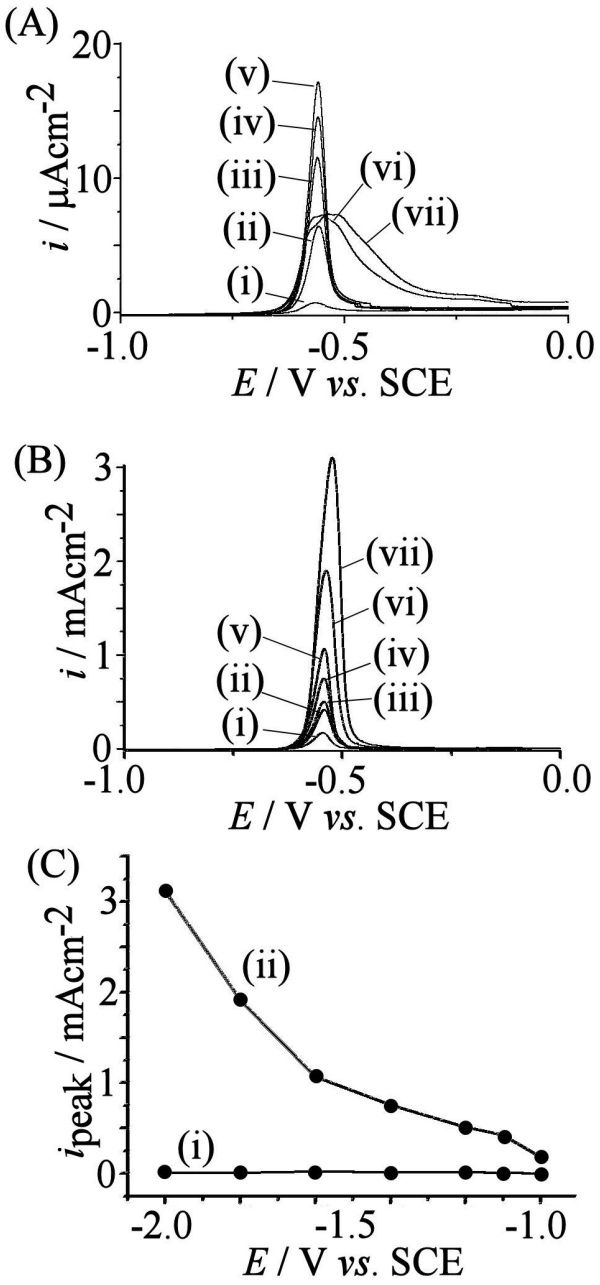

Figure 3. (A) Linear scan voltammograms (scan rate 0.1 Vs^{-1}, deposition potential (i) -1.0, (ii) -1.1, (iii) -1.2, (iv) -1.4, (v) -1.6, (vi) -1.8, and (vii) -2.0 V *vs*. SCE, deposition time 30s) for the stripping of iron deposited in 10 μM FeF_6^{3-} in 1 M NH_4F at a 3 mm diameter boron-doped diamond electrode. (B) Conditions as in (A) but with 8 Wcm^{-2} ultrasound (5 mm horn to electrode distance) applied. (C) Plot of the peak current for the iron stripping response versus deposition potential for (i) silent conditions and (ii) ultrasound conditions.

The plot in Figure 3C demonstrates the strong effect of ultrasonic agitation and the continuing increase of the stripping response at more negative deposition potentials.

The effect of the deposition time has been investigated in the absence and in the presence of ultrasound. Figure 4 clearly demonstrates the effect of continuing deposition, in particular with fast mass transport. The iron stripping peak is significantly further increased.

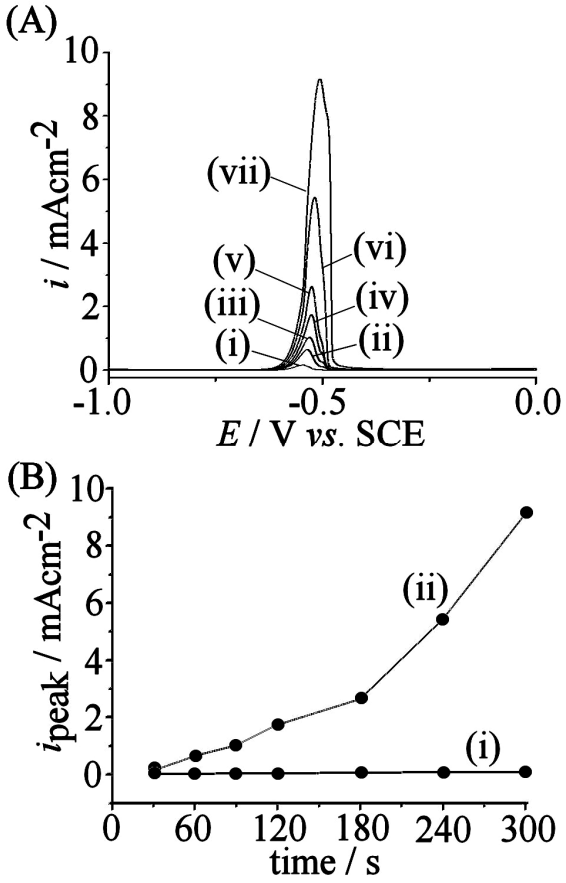

Figure 4. (A) Linear scan voltammograms (scan rate 0.1 Vs^{-1}, deposition potential -1.5 V *vs*. SCE, deposition time (i) 30, (ii) 60, (iii) 90, (iv) 120, (v) 180, (vi) 240, and (vii) 300s) for the stripping of iron deposited in 10 μM FeF_6^{3-} in 1 M NH_4F at a 3 mm diameter boron-doped diamond electrode. (B) Plot of the peak current for iron stripping versus deposition time.

In order to image the deposit formed under optimized conditions, SEM images of the boron-doped diamond surface with iron deposit were obtained. Figure 5 shows images in which a scratch line allows the boron-doped diamond base to be distinguished from the deposit. A nanoparticulate material with approximately 20-30 nm particle

diameter is observed after 600s deposition at -1.5 V vs. SCE in a solutions containing 10 μM FeF_6^{3-} and 1 M NH_4F.

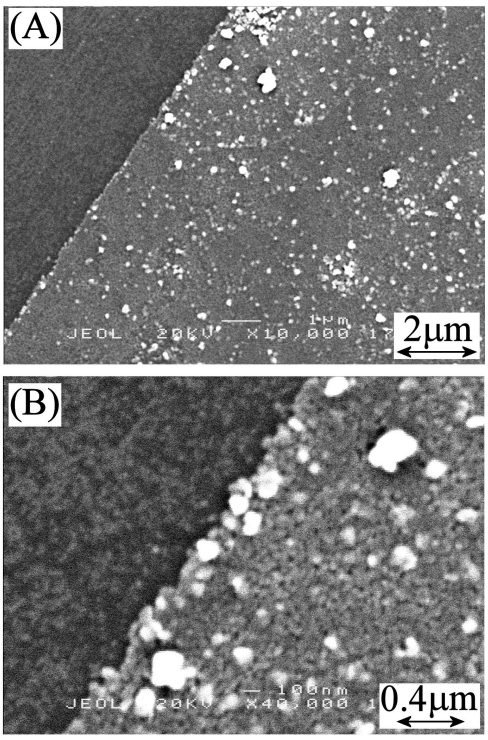

Figure 5. (A) Scanning electron micrographs for an iron deposit on boron doped diamond (generated by deposition at -1.5 V vs. SCE for 600s with 8 Wcm^{-2} ultrasound immersed in 10 mM FeF_6^{3-} in 1 M NH_4F. (B) Higher magnification image showing individual nanoparticles. Samples were scratched and gold sputter coated prior to imaging to improve image quality.

3.3. The Electro-Deposition and Stripping of Iron: Concentration Effects

Next, the effect of the iron concentration on the electro-deposition and stripping processes is investigated. Rather than going to lower iron levels, the effects of a higher iron concentration are explored innitially. Figure 6A shows linear scan voltammograms obtained after 30s deposition and for various levels of FeF_6^{3-} concentrations. Overall a complex behaviour is observed although the stripping peak clearly increases with FeF_6^{3-} concentration.

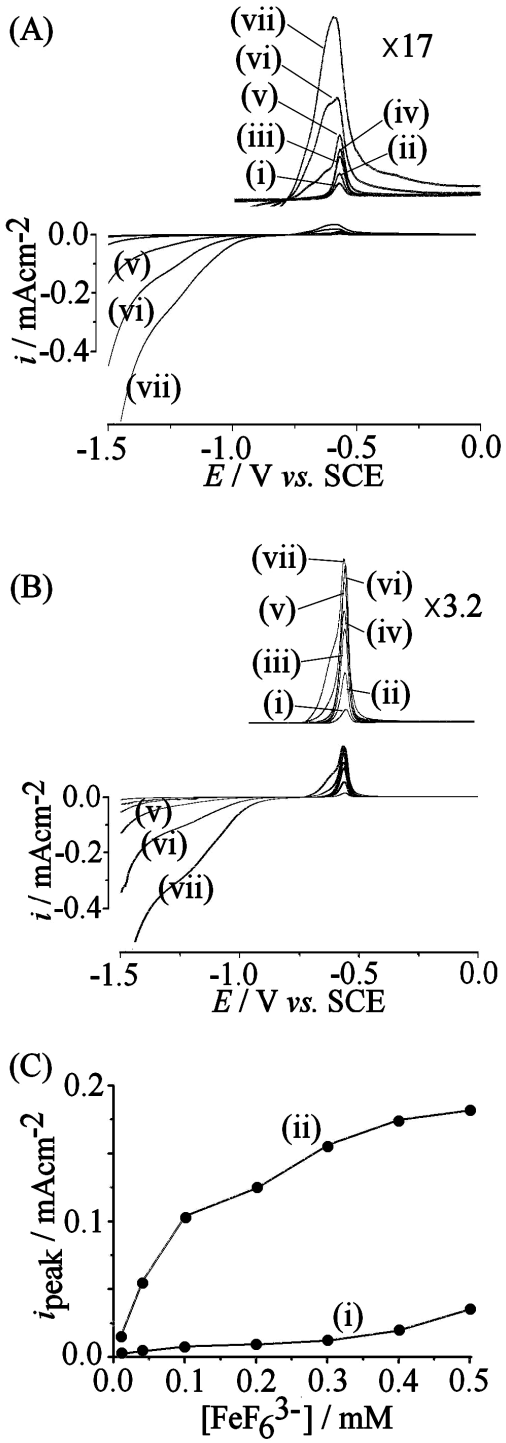

Figure 6. (A) Linear scan voltammograms (scan rate 0.1 Vs^{-1}, deposition potential -1.5 V *vs*. SCE, deposition time 30s) for the stripping of iron deposited in (i) 10, (ii) 40, (iii) 100, (iv) 200, (v) 300, (vi) 400, and (vii) 500 μM FeF_6^{3-} in 1 M NH_4F at a 3 mm diameter boron-doped diamond electrode. (B) Conditions as in (A) but with 8 Wcm^{-2} ultrasound (5 mm electrode to horn distance) applied. (C) Plot of the peak current for iron stripping versus FeF_6^{3-} concentration.

Increasing the FeF_6^{3-} concentration initially results in a simple increase in the stripping current peak. However, at concentration of 0.3 mM and above the shape of the peak is changed and the stripping process appears to commence already at a more negative potential. Closer inspection of Figure 6A shows that there is a distinct point at ca. -0.6 V vs. SCE where the current crosses from negative to positive. The presence of a higher concentration of FeF_6^{3-} appears to enhance the electro-dissolution kinetics for iron. The mechanism for this process is currently not well understood and additional work for example with quartz crystal microbalance mass sensors or spectro-electrochemical tools would provide further insight.

3.4. Catalytic Reactivity of Electro-Deposited Iron Towards Trichloroacetate

Iron is a highly catalytic metal with applications in a wide range of processes [12]. Often the state of the iron or iron oxide surface is important for controlling reactivity. Dehalogenation processes have been reported at iron metal particles [13] as well as at reduced forms of iron metal complexes such as hemin [14] or hemoglobin [15]. Here, the reduction of the trichloroacetate anion may be regarded as a model system for the reductive dehalogenation process at iron surfaces.

In Figure 7A cyclic voltammograms are shown recorded at a 3 mm diameter boron-doped diamond electrode immersed in a solution of 10 μM FeF_6^{3-} in 1 M NH_4F in the absence (i) and in the presence (ii) of 1 mM trichloroacetate. In the absence of FeF_6^{3-} no reduction response is observed even in the presence of higher concentration of trichloroacetate. The cathodic current in Figure 7A(ii) is therefore catalytic.

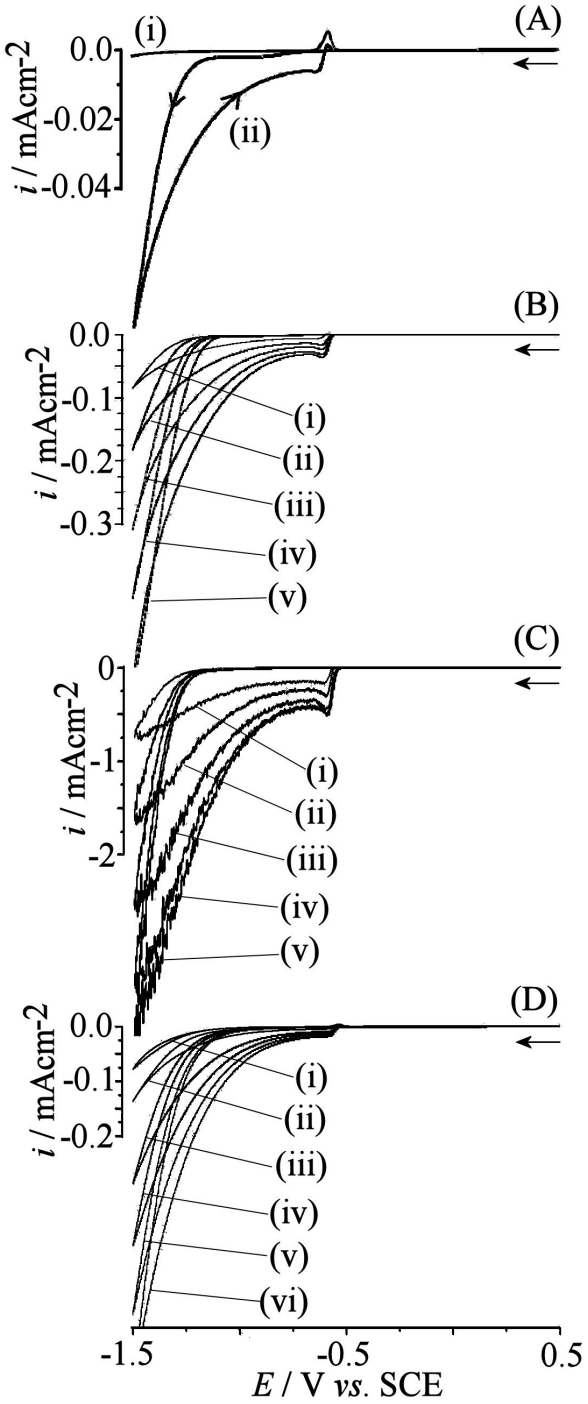

Figure 7. (A) Cyclic voltammograms (scan rate 0.02 Vs^{-1}) for the reduction and re-oxidation of 10 μM FeF_6^{3-} in 1 M NH_4F at a 3 mm diameter boron-doped diamond electrode (i) without and (ii) with 1 mM trichloroactate. (B) Conditions as in (A) and with (i) 1 mM, (ii) 2 mM, (iii) 3 mM, (iv) 4 mM, and (v) 5 mM trichloroacetate added. (C) Conditions as in (B) but in the presence of ultrasound (8 Wcm^{-2}, 5 mm electrode to horn distance). (D) Cyclic voltammograms (scan rate 0.02 Vs^{-1}) for the reduction and re-oxidation of immobilized iron at a 3 mm diameter boron-doped diamond electrode in 1 M NH_4F in the presence of (i) 0 mM, (ii) 1 mM, (iii) 3 mM, (iv) 5 mM, (v) 7 mM, and (vi) 9 mM trichloroactate.

It can be seen that the trichloroacetate reduction commences at a potential of ca. -0.8 V vs. SCE and then with increasing deposition of iron the current increases (see figure 7B). In the presence of ultrasound cathodic currents are further increased (see Figure 7C). It is very interesting to see the cathodic peak feature at ca. -0.6 V vs. SCE which is indicating a higher catalytic activity close to the potential where iron stripping is observed. The noise level on the sonovoltammograms for trichloroactetate reduction is relatively low consistent with a process dominated by the kinetics of a reaction step rather than by mass transport. The highest cathodic current observed for the reduction of 1 mM trichloroacetate, -0.75 mA cm^{-2}, is at least approximately consistent with a process with $n \approx 1$ (using equation 1). However, further experiments with dichloroacetate and monochloroacetae (not shown) also result in catalytic cathodic currents in the presence of iron and therefore (consistent with literature reports []) a stepwise reduction and dechloronation down to acetate (equation 5) is likely to occur overall.

$$Cl_3CCO_2^-(aq) + 3\ H_2O + 6\ e^- \rightleftharpoons H_3CCO_2^-(aq) + 3\ Cl^-(aq) + 3\ OH^- \quad (5)$$

Perhaps surprisingly, the catalytically active deposit of iron is not fully removed during the anodic stripping process. The passivation of the iron deposit appears to be facile and the removal of all iron from the electrode surface required a special cleaning procedure (see Experimental) based on dithionite and EDTA. This observation is consistent with a strongly adhering catalyst film at the boron-doped diamond electrode surface. Indeed, experiments with a iron-modified boron-doped diamond electrode in trichloroacetate containing solution (see Figure 7D) demonstrates that current similar to those obtained int eh presence of FeF63- are

obtained. Therefore, this kind of electrode remains catalytically active and it will be possible to transfer the catalyst-modified electrode into a wider range of solutions without fluoride and for a wider range of catalytic dehalogenation processes.

4. Conclusions

It has been demonstrated that iron is reversibly electrodeposited and stripped at boron-doped diamond electrodes immersed into aqueous 1 M NH_4F solution. A very sensitive stripping response is obtained even at very low concentrations of FeF_6^{3-} and the effects of concentration, deposition time, and deposition potential have been reported. The iron deposit has been demonstrated to provide electro-catalytic activity towards cathodic dehalogenation processes. Processes such as the reduction of trichloroacetate are facile in the presence of iron at the boron-doped diamond electrode surface. Further work on this system for potential analytical applications and on the benefits of iron for clean sonoelectrocatalytic dehalogenation or decontamination processes is in progress.

5. Acknowledgements

This work was supported by the EU COST Programme (Action D32, working groups ‘‘Microwave and Ultrasound Activation in Chemical Analysis’’ and ‘‘Electrochemistry with Ultrasound’’). V.S. and J.G.-G. thank the Generalidad Valenciana for the financial support by the Project GV05/104.